HHS Public Access

Author manuscript

Biomaterials. Author manuscript; available in PMC 2020 November 01.

Published in final edited form as:

Biomaterials. 2019 November ; 221: 119410. doi:10.1016/j.biomaterials.2019.119410.

Fluorocapsules Allow *In Vivo* Monitoring of the Mechanical Stability of Encapsulated Islet Cell Transplants

Dian R. Arifin[1,2], **Mangesh Kulkarni**[1,2], **Deepak Kadayakkara**[1,2,3], **Jeff W.M. Bulte**[*,1,2,3,4,5]

[1]Russell H. Morgan Department of Radiology and Radiological Science, Division of MR Research, the Johns Hopkins University School of Medicine, Baltimore, MD, 21205, USA.

[2]Cellular Imaging Section and Vascular Biology Program, Institute for Cell Engineering, the Johns Hopkins University School of Medicine, Baltimore, MD, 21205, USA.

[3]Department of Oncology, the Johns Hopkins University School of Medicine, Baltimore, MD, 21205, USA.

[4]Department of Chemical & Biomolecular Engineering, the Johns Hopkins University Whiting School of Engineering, Baltimore, MD, 21218.

[5]Department of Biomedical Engineering, the Johns Hopkins University School of Medicine, Baltimore, MD, 21205, USA.

Abstract

Clinical trials that have used encapsulated islet cell therapy have been few and overall disappointing. This is due in part to the lack of suitable methods to monitor the integrity vs. rupture of transplanted microcapsules over time. Fluorocapsules were synthesized by embedding emulsions of perfluoro-15-crown-5-ether (PFC), a bioinert compound detectable by ^{19}F MRI, into dual-alginate layer, Ba^{2+}-gelled alginate microcapsules. Fluorocapsules were spherical with an apparent smooth surface and an average diameter of 428 ± 52 μm. After transplantation into mice, the ^{19}F MRI signal of capsules remained stable for up to 90 days, corresponding to the total number of intact fluorocapsules. When single-alginate layer capsules were ruptured with alginate lyase, the ^{19}F MRI signal dissipated within 4 days. For fluoroencapsulated *luciferase*-expressing mouse ßTC6 insulinoma cells implanted into autoimmune NOD/Shiltj mice and subjected to alginate-lyase induced capsule rupture *in vivo*, the ^{19}F MRI signal decreased sharply over time along with a decrease in bioluminescence imaging signal used as measure of cell viability *in vivo*. These results indicate that maintenance of capsule integrity is essential for preserving transplanted cell survival, where a decrease in ^{19}F MRI signal may serve as a predictive imaging surrogate biomarker for impending failure of encapsulated islet cell therapy.

[*]Corresponding Author: Jeff W.M. Bulte, Ph.D., Department of Radiology, The Johns Hopkins University School of Medicine, Miler Research Building Rm 659, 733 N Broadway, Baltimore, MD 21205, Phone: 443-287-0996, Fax: 443-287-7945, jwmbulte@mri.jhu.edu.

Data availability

The raw/processed data required to reproduce these findings cannot be shared at this time due to technical or time limitations.

Keywords

Islet cell transplantation; encapsulation; diabetes; magnetic resonance imaging

1. Introduction

Type I diabetes mellitus (T1DM) is a result of autoimmune destruction of the insulin-producing beta cells in the pancreas. In encapsulated islet therapy, damaged beta cells in T1DM patients are replaced with healthy donor islets immunoprotected inside selectively permeable alginate hydrogel microcapsules. Many studies have reported that this approach can successfully restore normoglycemia or reduced insulin requirements in diabetic rodents [1, 2] and primates [3–5] without the use of immunosuppressive drugs, but the less favorable outcomes of clinical trials indicate that further development of capsule technology is necessary for further translation [6–9]. For example, in one of the few clinical studies performed, a patient received four allografts of encapsulated human islets without immunosuppressants, and a reduction in insulin dose or glycemic control was not achieved even though human c-peptide was detectable up to 2.5 years post-transplantation [10, 11]. Human c-peptide levels in three other patients receiving one or two allografts were undetectable at 1–4 weeks. The underlying causes of the graft failure are not known, calling for approaches to interrogate the fate of encapsulated islet cells once they are transplanted.

Among the many factors critical for the success of encapsulated islet therapy, the mechanical stability of the capsules relates directly to their immunoprotective capacity, as ruptured capsules may expose the encapsulated islets to the hostile host environment. Microcapsules must be strong enough to survive the shearing forces encountered during the transplantation procedure as well as changes in the graft site microenvironment during and after transplantation. Indeed, improving the design and/or biomaterials of capsules in order to further strengthen and stabilize the capsules has been the focus of recent studies [12–17]. Methods to evaluate the mechanical strength and stability of the capsules *in vitro* are numerous, for example bead agitation, osmotic pressure, rotational stress, and compression testing [12, 18–20]. However, clinically relevant and non-invasive ways to assess the integrity of transplanted capsules *in vivo* have not yet been developed, with explantation of capsule grafts followed by *in vitro* examination being the only available technique at present [21]. This invasive technique does not allow longitudinal or real-time monitoring of the time course of disintegration, and cannot report on the capsule condition at the graft site *in situ*, aside from the presence of damaged or deformed capsule artifacts due to the explantation procedure.

In this study, we investigated whether the mechanical stability of alginate microcapsules can be non-invasively assessed with ^{19}F magnetic resonance imaging (MRI). To this end, we added perfluoro-15-crown-5-ether (PFC) to the alginate hydrogel to create fluorocapsules [22]. PFC is a bioinert compound with 20 equivalent ^{19}F nuclei that give rise to a single NMR peak, and can be used as a tracer to produce “hot spots” on ^{19}F MRI without background signal [23]. We hypothesize that fluorocapsules with a compromised mechanical stability release their PFC tracer *in vivo* which is subsequently rapidly cleared by the body

in gaseous form via exhalation, while intact fluorocapsules retain the PFC tracer. The leakage and dissipation of PFC tracer from ruptured fluorocapsules may then non-invasively detected with ^{19}F MRI as a decrease in ^{19}F MRI signal, while the ^{19}F MRI signals of intact fluorocapsules would remain stable. As a proof of concept, we compared two types of fluorocapsules with opposite mechanical stabilities. Strong, dual-layer fluorocapsules were prepared using clinical grade protamine sulfate as cross-linker and barium ions for alginate gelation [12]. To create weak fluorocapsules, we synthesized single layer fluorocapsules using calcium ions to gel the alginate, which can be readily ruptured by addition of alginate lyase. Furthermore, since capsule rupture would no longer physically immunoprotect encapsulated islet cells, we performed bioluminescent imaging (BLI) to correlate islet cell viability to the magnitude of the ^{19}F MRI signal. As capsule rupture would precede immunodestruction followed by cell death, we investigated if the ^{19}F MRI outcome could possibly serve as a surrogate biomarker for encapsulated cell survival.

2. Results and Discussion

2.1. Characterization of fluorocapsules

We previously reported that dual-alginate layer microcapsules gelled by Ba^{2+} ions and cross-linked with protamine sulfate (alginate-protamine sulfate-alginate or APSA) exhibit superior mechanical strength compared to commonly used Ca^{2+}-gelled alginate microcapsules [12]. APSA+PFC fluorocapsules were successfully synthesized with a spherical shape, apparent smooth surface and an average diameter of 428 ± 52 μm. This size was not statistically different from APSA (unlabeled) microcapsules, which was 444 ± 21 μm [12]. Compared to unlabeled microcapsules, fluorocapsules appeared dark in color due to the encapsulated PFC emulsion (Fig. 1a,b). Each fluorocapsule contained $5.03\pm3.00\times10^{17}$ ^{19}F atoms, appearing as a single peak on the NMR spectrum (Fig. 1c).

Two different *in vitro* tests were performed to evaluate the mechanical strength of the fluorocapsules against possible physical changes in the tissue microenvironment that the microcapsules might be exposed to upon transplantation (Fig. 1d,e). Labeling the microcapsules with PFC did not alter their mechanical strength as compared to unlabeled microcapsules. Fluorocapsules were significantly stronger ($p<0.01$) than commonly used alginate microcapsule gelled by 100 mM Ca^{2+} and cross-linked by poly-L-lysine (APLLA capsules) in withstanding compression forces or a changes osmotic pressure.

2.2. ^{19}F MRI of fluorocapsules

In vitro ^{19}F MRI demonstrated that dual-alginate layer fluorocapsules could be imaged at a sensitivity level of single capsules (Fig. 2a,b). The total ^{19}F nuclei per voxel (normalized to the TFA reference, Fig. 2c) in 1:10 fluorocapsules was 4.0:48.5. Five thousand dual-layer empty fluorocapsules (without cells) transplanted into the peritoneal cavity of a C57/Bl6 mouse did not exhibit ^{1}H signal *in vivo* (Fig. 1d), and hence could not be distinguished from the host tissue. In contrast, fluorocapsules were easily detected on ^{19}F MRI as “hot spots”, and single capsules could be detected *in vivo* (Fig. 2d–f)

For ^{1}H MRI, alginate microcapsules have previously been labeled with metallic contrast agents including iron oxide nanoparticles[24–26] and gadolinium nanoparticles [1, 27], where they appear as hypointense or hyperintense contrast against background tissue, respectively. However, other sources of endogenous contrast may exist in the peritoneum, such as air and stool in the colon (dark appearance) or fatty tissue (bright appearance), rendering it difficult to identify and discern the capsule implants against the tissue background. A main advantage of ^{19}F MRI is that fluorine is not a contrast agent but a tracer that is detected directly, and thus can be imaged as “hot spots” [28] due to the negligible amount of fluorine agents in the tissues, much like PET or SPECT imaging using radiotracers. As shown in Figure 1, it is impossible to detect the distribution of microcapsules *in vivo* using only ^{1}H MRI.

In order to study the stability of dual-alginate layer fluorocapsules *in vivo*, we subcutaneously engrafted fluorocapsules into C57/Bl6 mice and imaged them for 90 days (Fig. 3a). The total ^{19}F nuclei/voxel in the implant, normalized to the reference, did not show significant differences for 90 days. Representative overlaid ^{1}H/^{19}F MRI of mice at day 1 and day 90 post-transplantation (Fig. 3b and c, respectively) showed water in the subcutaneous pouch at day 1 as high signal intensity on the ^{1}H image, which was completely absorbed by the body by day 90. The implanted fluorocapsules remained localized within the pouch up to day 90.

2.3. *In vitro* MRI of fluorocapsule rapture

As a proof-of-concept that ruptured fluorocapsules could be detected as a decrease in ^{19}F MR-signal, we prepared weak single-layer fluorocapsules that could be enzymatically digested by alginate lyase. Microscopic images of fluorocapsules before and after rupture are presented in Fig. 4a,b. ^{1}H MRI was not able to distinguish intact from ruptured fluorocapsules (Fig. 4c,d). In contrast, the ^{19}F MR signal intensity of fluorocapsule phantoms decreased after rupture (Fig. 4e,f). The total ^{19}F nuclei/voxel (normalized to a reference) in the fluorocapsule phantoms reduced from 2.33×10^{2} to 1.42×10^{2} after rupture.

2.4. *In vivo* imaging of fluorocapsule rapture and encapsulated cell survival

To demonstrate the ability of ^{19}F MRI to detect capsule rupture *in vivo*, and its association with cell death resulting from loss of immunoprotection, we transplanted fluoroencapsulated *luciferase*-transfected mouse insulinoma cells subcutaneously into diabetic NOD/Shiltj mice. Transplanting the fluorocapsules into a subcutaneous site constrained the capsules to one particular graft location for the duration of the experiment, and thus enabled reproducible sampling of the entire graft site by ^{19}F MRI and BLI at different time points. Although intraperitoneal transplantation is typically used to effectively treat diabetic mice [1, 2], we decided to forego this graft site since fluorocapsules would disperse as single entitities throughout the peritoneal cavity, making it difficult to serially image the engrafted fluorocapsules.

One day after grafting, capsules were subjected to rupture by alginate lyase injection. We first assessed whether alginate lyase incubation itself would have an adverse effect on cell viability. An MTS assay of *luciferase*-mouse insulinoma cells, cultured with alginate lyase at

the same concentration as cells were exposed to *in vivo*, showed that this enzyme treatment did not affect cell viability and proliferation (Fig. 5).

Fig. 6 shows *in vivo* $^{1}H/^{19}F$ overlay MRI and BLI images of the various transplantation paradigms at day 1 and day 4 after transplantation. The decrease in ^{19}F MR signal after weak single-alginate layer fluorocapsule rupture occurred concurrently with a decrease in cell viability as measured by BLI (Fig. 7a), with a good agreement between the ^{19}F MR and BLI signal intensity from pre- to post-rupture. For comparison, we also imaged single-alginate layer fluoroencapsulated cells without lyase administration (i.e., intact single-alginate layer fluorocapsules) and unencapsulated cell implants ate the same time as for the ruptured single-alginate layer fluorocapsules (day 1 and 4 post-engraftment). Fig. 7b,c, shows that the ^{19}F signal and BLI signal intensity of intact single-alginate layer fluorocapsules remained stable for at least 4 days after transplantation, while the BLI signal of unencapsulated cells sharply decreased after transplantation. Hence, both the presence and preservation of capsule integrity is necessary for maintaining cell survival. These results indicate that the ^{19}F signal may serve as an early predictive marker for cell survival, with capsule rupture preceding cell death. As ^{19}F tracer-based MRI does not interfere with ^{1}H-based MRI (unlike the use of metallic contrast agents), this imaging approach may be further combined with ^{1}H-based magnetization transfer ratio imaging to study the presence of a peri-capsular host immune reaction [29].

Fluorocapsules have translational potential for clinical applications as potentially toxic metal-based contrast agents are not used in the formulation. Gadolinium-chelate contrast agents have been reported to cause nephrogenic systemic fibrosis in patients with impaired renal function where they remain for prolonged times in the body [30]. Exposure of iron oxide nanoparticles to cells may induce toxic effects [31–33]. PFC, on the other hand, is a bioinert compound that was originally developed as a clinical artificial blood substitute for oxygen transport applications [34–37]. Moreover ^{19}F-based tracers have recently obtained IND status for MRI clinical cell tracking applications [38, 39]. Due to its hydrophobicity, PFC must be emulsified using egg yolk-derived lecithin and safflower oil for stable and homogeneous incorporation and distribution inside alginate microcapsules. Both egg lecithin and safflower oil are FDA-approved products and are commonly used in food, pharmaceutical products and cosmetics.

3. Conclusion

In this report, we present proof-of-concept that fluorocapsules allow “hot spot” imaging of the distribution and mechanical stability of encapsulated islet cell transplants *in vivo* using ^{19}F MRI. When engrafted fluorocapsules were ruptured *in vivo*, their PFC tracer was released and subsequently cleared from the graft site. This event was manifested as a decrease in ^{19}F MRI signal. In contrast, the signals of intact fluorocapsule grafts remained stable for at least 90 days *in vivo*. The use of fluorocapsules may provide a clinically relevant, quantitative and non-invasive strategy to monitor the mechanical stability of the capsules *in vivo* in a serial and real-time fashion. Since ruptured fluorocapsules lead to islet rejection, our fluorocapsule approach may be used as a surrogate marker to monitor and predict islet graft rejection and therefore impending failure of encapsulated islet therapy.

4. Experimental Section

4.1. Fluorocapsule synthesis and cell encapsulation

To prepare PFC emulsions, egg yolk lecithin (5% w/v, Sigma Aldrich, St. Louis, MO) and safflower oil (2% v/v, Sigma Aldrich) in sterile deionized water were sonicated on ice at 40% amplitude for 10 minutes. PFC (MW=580.01 Da, Oakwood Chemical, West Columbia, SC) was mixed with the lipid mixture (20% v/v) and then sonicated again on ice at 40% amplitude for 10 minutes. Two types of alginate were purchased from Novamatrix (Sandvika, Norway): 1) Pronova ultrapure low-viscosity high-guluronate (UP LVG) alginate, where > 60% of the monomer units are guluronate; and 2) Pronova low-viscosity high-mannuronate (UP LVM) alginate, where >50% of the monomer units are mannuronate. Both alginates have a MW=75–200 kDa, endotoxin level ≤ 100 EU/g and viscosity = 20–200 mPas.

PFC emulsions were immediately mixed with UP LVG alginate to obtain a final alginate and PFCconcentration of 2% and 6% v/v, respectively [40]. For cell encapsulation, *luciferase*-mouse βTC6 insulinoma cells (1000 cells per capsule on average, ATCC, Manassas, VA) were suspended in the PFPE/alginate mixture. The capsules were produced with an electric bead generator technique using a 20 mM $BaCl_2$ gelation bath. Capsules were washed twice with sterile 0.9% NaCl and 10 mM HEPES, and then cross-linked with clinical grade 0.05%w/v protamine sulfate (MW=4500 Da, NovaPlus, APP Pharmaceuticals, Schaumburg, IL) for 10 minutes on a horizontal rocker. After saline washing, the capsules were finally coated with 0.15% w/v UP LVM alginate for 10 minutes as the second alginate layer. Capsules were washed with saline twice before being further used. “Weak” single alginate-layer fluorocapsules were created by gelling the capsules using 50 mM $CaCl_2$ without protamine sulfate cross-linker and without a final LVM alginate layer. Unless otherwise specified, solutions were prepared in filtered 0.9% NaCl and 10 mM HEPES.

4.2. Characterization of fluorocapsules

4.2.1. *In vitro* assessment of mechanical strength: Osmotic pressure test—

One hundred capsules (n=3 independent experiments) were washed with picopure water and incubated in 5 mL of picopure water at 37°C for 1 hour. Capsules were then washed with 0.9% NaCl/10 mM HEPES and stained with 0.4% trypan blue for 5 minutes to aid visualization of capsule fracture. After subsequent saline washing, fractured and intact capsules were counted using an inverted light microscope (Olympus IX71, Center Valley, PA).

4.2.2. *In vitro* assessment of mechanical strength: Compression test.—

The mechanical strength of the capsules was quantified with a Texture Analyzer XT plus (Stable Micro Systems, Godalming, UK) equipped with a force transducer with a resolution of 1 mN. Texture Exponent software version 6.0 was used for recording and analyzing data. The equipment consisted of a mobile probe (P/25L) moving vertically with a pre-test speed of 0.5 mm/s, a test speed of 0.01 mm/s, and a post-test speed of 2 mm/s. The mechanical strength was measured by compressing a group of ten microcapsules (n=3 independent experiments) using a uniaxial compression test. The force (expressed in grams) was

quantified when a compression of 60% was reached [41]. The probe was set to return to the original position immediately after compression.

4.2.3. Quantification of ^{19}F atoms per fluorocapsule.—

100 fluorocapsules (n=3 indepenent experiments) were ruptured by 0.5 M EDTA at pH=8.0, and the resulting mixture was measured at 400 MHz using a Varian NMR system (Palo Alto, CA) using 0.1% trifluoroacetic acid as reference.

4.3. Imaging fluorocapsules with ^{1}H/^{19}F MRI and BLI

For *in vitro* MRI of intact capsules, one and ten fluorocapsules were suspended in 2% agarose and imaged using a 17.6 T vertical bore scanner (Bruker Biospin, Erlangen, Germany) and a dual-tunable ^{19}F/^{1}H birdcage resonator coil with a 25 mm inner diameter. A rapid acquisition with relaxation enhancement (RARE) pulse sequence was used for ^{1}H/^{19}F MRI with the following parameters: Repetition time (TR)=4/1s, echo time (TE)=58/6 ms, matrix=128×128/128×128, slice thickness (ST)=1/1 mm, number of averages (NA)=2/4, and field of view (FOV)=2×2/2×2 cm.

For *in vitro* MRI of ruptured fluorocapsules, 3000 capsules were incubated at 37°C in 0.9% NaCl and 10mM HEPES containing alginate lyase (0.075 mg/ml, Sigma Aldrich) for 2 days to weaken the capsules. Capsules were passed through a 25G needle to rupture them. Intact and ruptured fluorocapsules were loaded into 5-mm NMR glass tubes and imaged as described above using the following parameters: TR=0.5/1 s, TE=11/15 ms, ST=5/5 mm, matrix=96×96/128×128, NA=4/4, and FOV=2×2/2×2 cm.

For *in vivo* MRI of intact fluorocapsules, 5000 fluorocapsules were transplanted into the peritoneal cavity of a C57/Bl6 mouse (Jackson Laboratories, Bar Harbor, ME) to demonstrate the imaging sensitivity at this site. To measure their *in vivo* stability, 5000 empty fluorocapsules were implanted subcutaneously (s.c.) into normal C57Bl/6J mice (n=5). ^{1}H/^{19}F MRI was performed using a 11.7T horizontal scanner (Bruker Biospin) and a dual-tunable ^{19}F/^{1}H surface coil with a 20 mm inner diameter. MRI was performed at day 1 post-engraftment, every week for 30 days and at day 60 and 90. The RARE parameters for ^{1}H/^{19}F MRI of animals were TR=4/1 s, TE=30/23 ms, ST=2/2 mm, matrix=196×128/196×128, NA=4/4, and FOV=3.2×2/3.2×2 cm. A liquid PFC sample inside a capillary tube was used as reference. Mean ^{19}F MRI signals were quantified using Voxel Tracker software (Celsense, Pittsburgh, PA). Data are reported as the ratio of the total ^{19}F nuclei/voxel in the implants vs. the mean^{19}F nuclei/voxel in the reference.

For luciferase transduction of mouse βTC6 insulinoma cells, packaged lentivector (pLenti4-CMV-fLuc2, 250 μl/ml media) and polybrene (6 μg/ml media) were added to cells at 80% confluency in order to achieve a multiplicity of infection of 10. The medium was changed after 24 hour incubation, followed by cell expansion to yield the desired cell numbers.

For *in vivo* imaging of ruptured fluorocapsules, 5000 weak (single-layer) fluoroencapsulated luciferase-transduced mouse insulinoma cells were engrafted s.c. into diabetic NOD/Shiltj mice (Jackson Laboratories, n=6). Alginate lyase (1.2 mg in 100 μl PBS, Sigma Aldrich) was injected into the implant site at one day post-transplantation in order to rupture the

fluorocapsules. BLI was performed to assess *in vivo* cell survival using an IVIS Spectrum/CT scanner (Perkin-Elmer, Waltham, MA). $^{1}H/\ ^{19}F$ MRI was performed before and after lyase injection (day 1 and 4 after transplantation, respectively). Mice engrafted with weak fluoroencapsulated cells without lyase injection (n=5) or unencapsulated cells (n=5) served as controls, using the same imaging and signal processing protocols.

4.4. Toxicity studies of using alginate lyase

Mouse insulinoma cells were cultured with and without alginate lyase at the same concentrations used *in vivo*. Cell viability and proliferation were measured using a [3-(4,5-dimethylthiazol-2-yl)-5-(3-carboxymethoxyphenyl)-2-(4-sulfophenyl)-2H-tetrazolium] (MTS) assay (CellTiter 96 AQueous One Solution Cell Proliferation Assay, Promega, Madison, WI). Data were normalized to the values at day 1 post-culture.

4.6. Statistical analysis

Statistical differences were calculated by a two-tailed, unpaired, unequal variance student's t-test with a significance level of of $p<0.01$ or $p<0.05$.

Acknowledgements

This study was funded by Maryland Stem Cell Research Fund (MSCRFF-0035 and MSCRFI-0161), and the National Institutes of Health (R01 DK106972).

References

1. Arifin DR, et al., Trimodal gadolinium-gold microcapsules containing pancreatic islet cells restore normoglycemia in diabetic mice and can be tracked by using US, CT, and positive-contrast MR imaging. Radiology, 2011 260(3): p. 790–8. [PubMed: 21734156]
2. Kim J, et al., Multifunctional Capsule-in-Capsules for Immunoprotection and Trimodal Imaging. Angewandte Chemie, 2011 50(10): p. 2317–2321. [PubMed: 21351344]
3. Dufrane D, Goebbels RM, and Gianello P, Alginate macroencapsulation of pig islets allows correction of streptozotocin-induced diabetes in primates up to 6 months without immunosuppression. Transplantation, 2010 90(10): p. 1054–62. [PubMed: 20975626]
4. Safley SA, et al., Microencapsulated adult porcine islets transplanted intraperitoneally in streptozotocin-diabetic non-human primates. Xenotransplantation, 2018 25(6): p. e12450. [PubMed: 30117193]
5. Elliott RB, et al., Intraperitoneal alginate-encapsulated neonatal porcine islets in a placebo-controlled study with 16 diabetic cynomolgus primates. Transplant Proc, 2005 37(8): p. 3505–8. [PubMed: 16298643]
6. Orive G, et al., Engineering a Clinically Translatable Bioartificial Pancreas to Treat Type I Diabetes. Trends Biotechnol, 2018 36(4): p. 445–456. [PubMed: 29455936]
7. Smith KE, Johnson RC, and Papas KK, Update on cellular encapsulation. Xenotransplantation, 2018 25(5): p. e12399. [PubMed: 29732615]
8. Jacobs-Tulleneers-Thevissen D, et al., Sustained function of alginate-encapsulated human islet cell implants in the peritoneal cavity of mice leading to a pilot study in a type 1 diabetic patient. Diabetologia, 2013 56(7): p. 1605–14. [PubMed: 23620058]
9. Zamboni F and Collins MN, Cell based therapeutics in type 1 diabetes mellitus. Int J Pharm, 2017 521(1–2): p. 346–356. [PubMed: 28242376]
10. Tuch BE, et al., Safety and viability of microencapsulated human islets transplanted into diabetic humans. Diabetes Care, 2009 32(10): p. 1887–9. [PubMed: 19549731]

11. Cahill D, Zamboni F, and Collins MN, Radiological Advances in Pancreatic Islet Transplantation. Acad Radiol, 2019.
12. Arifin DR, et al., Microcapsules with intrinsic barium radiopacity for immunoprotection and X-ray/CT imaging of pancreatic islet cells. Biomaterials, 2012 33(18): p. 4681–9. [PubMed: 22444642]
13. Ma Y, et al., Modeling and optimization of membrane preparation conditions of the alginate-based microcapsules with response surface methodology. J Biomed Mater Res A, 2012 100(4): p. 989–98. [PubMed: 22307962]
14. Hillberg AL, et al., Encapsulation of porcine pancreatic islets within an immunoprotective capsule comprising methacrylated glycol chitosan and alginate. J Biomed Mater Res B Appl Biomater, 2014.
15. Zheng G, et al., Improving stability and biocompatibility of alginate/chitosan microcapsule by fabricating bi-functional membrane. Macromol Biosci, 2014 14(5): p. 655–66. [PubMed: 24436207]
16. Vaithilingam V, et al., Effect of prolonged gelling time on the intrinsic properties of barium alginate microcapsules and its biocompatibility. J Microencapsul, 2011 28(6): p. 499–507. [PubMed: 21827357]
17. Desai T and Shea LD, Advances in islet encapsulation technologies. Nat Rev Drug Discov, 2017 16(5): p. 338–350. [PubMed: 28008169]
18. Park JB, et al., Xenotransplantation of exendin-4 gene transduced pancreatic islets using multi-component (alginate, poly-L-lysine, and polyethylene glycol) microcapsules for the treatment of type 1 diabetes mellitus. J Biomater Sci Polym Ed, 2013 24(18): p. 2045–57. [PubMed: 23905775]
19. Bhujbal SV, et al., Factors influencing the mechanical stability of alginate beads applicable for immunoisolation of mammalian cells. J Mech Behav Biomed Mater, 2014 37: p. 196–208. [PubMed: 24951926]
20. Darabbie MD and Opara EC, Determination of the Mechanical Strength of Microcapsules. Methods Mol Biol, 2017 1479: p. 111–118. [PubMed: 27738930]
21. McQuilling JP, et al., Retrieval of Microencapsulated Islet Grafts for Post-transplant Evaluation. Methods Mol Biol, 2017 1479: p. 157–171. [PubMed: 27738934]
22. Barnett BP, et al., Fluorocapsules for improved function, immunoprotection, and visualization of cellular therapeutics with MR, US, and CT imaging. Radiology, 2011 258(1): p. 182–91. [PubMed: 20971778]
23. Ruiz-Cabello J, et al., Fluorine (19F) MRS and MRI in biomedicine. NMR Biomed, 2011 24(2): p. 114–29. [PubMed: 20842758]
24. Link TW, et al., MR-guided portal vein delivery and monitoring of magnetocapsules: assessment of physiologic effects on the liver. J Vasc Interv Radiol, 2011 22(9): p. 1335–40. [PubMed: 21816623]
25. Barnett BP, et al., Magnetic resonance-guided, real-time targeted delivery and imaging of magnetocapsules immunoprotecting pancreatic islet cells. Nat Med, 2007 13(8): p. 986–91. [PubMed: 17660829]
26. Arifin DR, et al., Magnetoencapsulated human islets xenotransplanted into swine: a comparison of different transplantation sites. Xenotransplantation, 2016 23(3): p. 211–21. [PubMed: 27225644]
27. Sarkis S, et al., Magnetic resonance imaging of alginate beads containing pancreatic beta cells and paramagnetic nanoparticles. ACS Biom. Sci. Eng, 2017 3(3576–3587).
28. Bulte JW, Hot spot MRI emerges from the background. Nat Biotechnol, 2005 23(8): p. 945–6. [PubMed: 16082363]
29. Chan KW, et al., Magnetization transfer contrast MRI for non-invasive assessment of innate and adaptive immune responses against alginate-encapsulated cells. Biomaterials, 2014 35(27): p. 7811–8. [PubMed: 24930848]
30. Thomsen HS, et al., Nephrogenic systemic fibrosis and gadolinium-based contrast media: updated ESUR Contrast Medium Safety Committee guidelines. Eur Radiol, 2013 23(2): p. 307–18. [PubMed: 22865271]
31. Singh N, et al., Potential toxicity of superparamagnetic iron oxide nanoparticles (SPION). Nano Rev, 2010 1.

32. Mahmoudi M, et al., Assessing the in vitro and in vivo toxicity of superparamagnetic iron oxide nanoparticles. Chem Rev, 2011 112(4): p. 2323–38. [PubMed: 22216932]
33. Kostura L, et al., Feridex labeling of mesenchymal stem cells inhibits chondrogenesis but not adipogenesis or osteogenesis. NMR Biomed, 2004 17(7): p. 513–7. [PubMed: 15526348]
34. Cabrales P and Intaglietta M, Blood substitutes: evolution from noncarrying to oxygen- and gas-carrying fluids. ASAIO J, 2013 59(4): p. 337–54. [PubMed: 23820271]
35. Torres LN, Spiess BD, and Torres Filho IP, Effects of perfluorocarbon emulsions on microvascular blood flow and oxygen transport in a model of severe arterial gas embolism. J Surg Res, 2013.
36. Habib FA and Cohn SM, Blood substitutes. Curr. Opin. Anaesthesiol, 2004 17(2): p. 139–143. [PubMed: 17021542]
37. Spahn DR, Blood substitutes. Artificial oxygen carriers: perfluorocarbon emulsions. Crit Care, 1999 3: p. R93–R97. [PubMed: 11094488]
38. Ahrens ET, et al., Clinical cell therapy imaging using a perfluorocarbon tracer and fluorine-19 MRI. Magn Reson Med, 2014 72(6): p. 1696–701. [PubMed: 25241945]
39. Rose LC, et al., Fluorine-19 Labeling of Stromal Vascular Fraction Cells for Clinical Imaging Applications. Stem Cells Transl Med, 2015 4(12): p. 1472–81. [PubMed: 26511652]
40. Barnett BP, et al., Synthesis of magnetic resonance-, X-ray- and ultrasound-visible alginate microcapsules for immunoisolation and noninvasive imaging of cellular therapeutics. Nat Protoc, 2011 6(8): p. 1142–1151. [PubMed: 21799484]
41. Bhujbal SV, et al., Factors influencing the mechanical stability of alginate beads applicable for immunoisolation of mammalian cells.S. Journal of the Mechanical Behavior of Biomedical Materials, 2014 37: p. 196–208. [PubMed: 24951926]

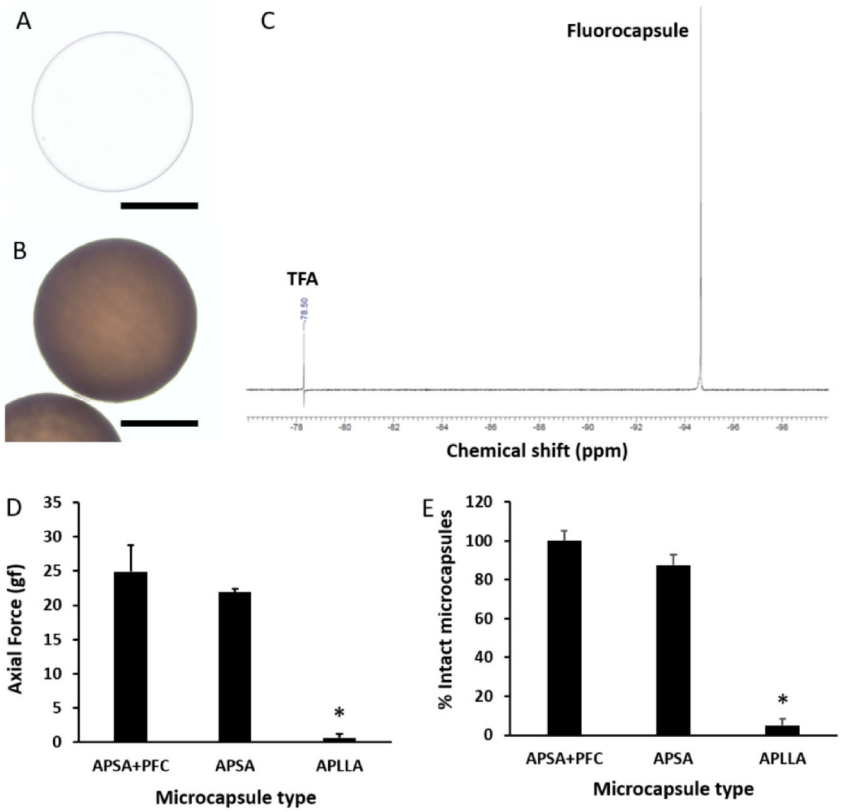

Fig. 1:

Light microscopic image of an unlabeled APSA microcapsule (a) and an APSA fluorocapsule (b). Scale bar = 200 μm. c) ^{19}F NMR spectrum (obtained at 400 MHz) of ruptured fluorocapsules showing a single peak. Trifluoroacetic acid (TFA) was used as reference. d) Axial force required to compress fluorocapsules (APSA+PFC), unlabeled APSA microcapsules and unlabeled APLLA microcapsules to 60% of their original size. e) Percentage of intact microcapsules after an osmotic pressure test. *p<0.01.

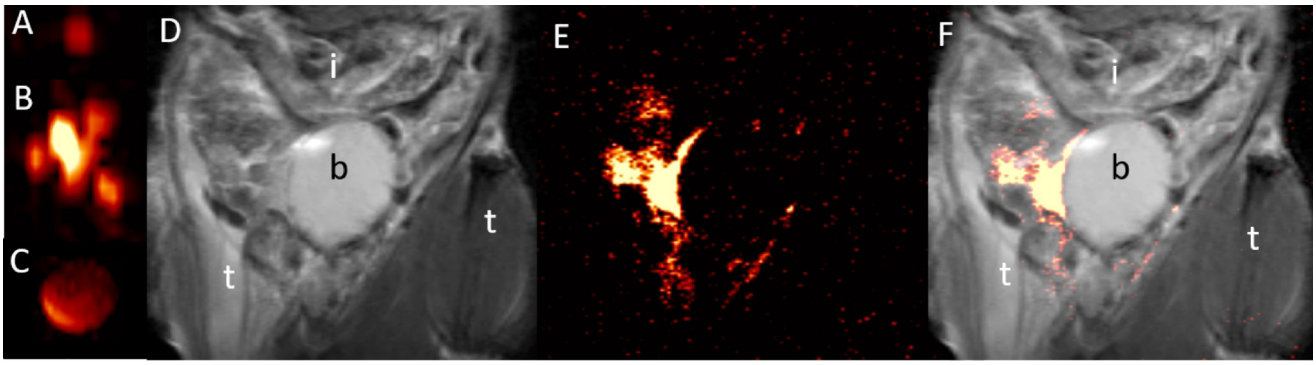

Fig. 2:

a,b) *In vitro* 17.6T ^{19}F MR images of 1 (a) and 10 (b) dual-alginate layer fluorocapsules and (c) reference (undiluted PFC emulsion). e). d-f) *In vivo* ^{1}H (d), ^{19}F (e) and overlaid ^{1}H/^{19}F (f) 11.7T MR images of intact fluorocapsules transplanted i.p. in a C57/Bl6 mouse at day 1 post-transplantation. i=intestines, b=bladder, t=thigh.

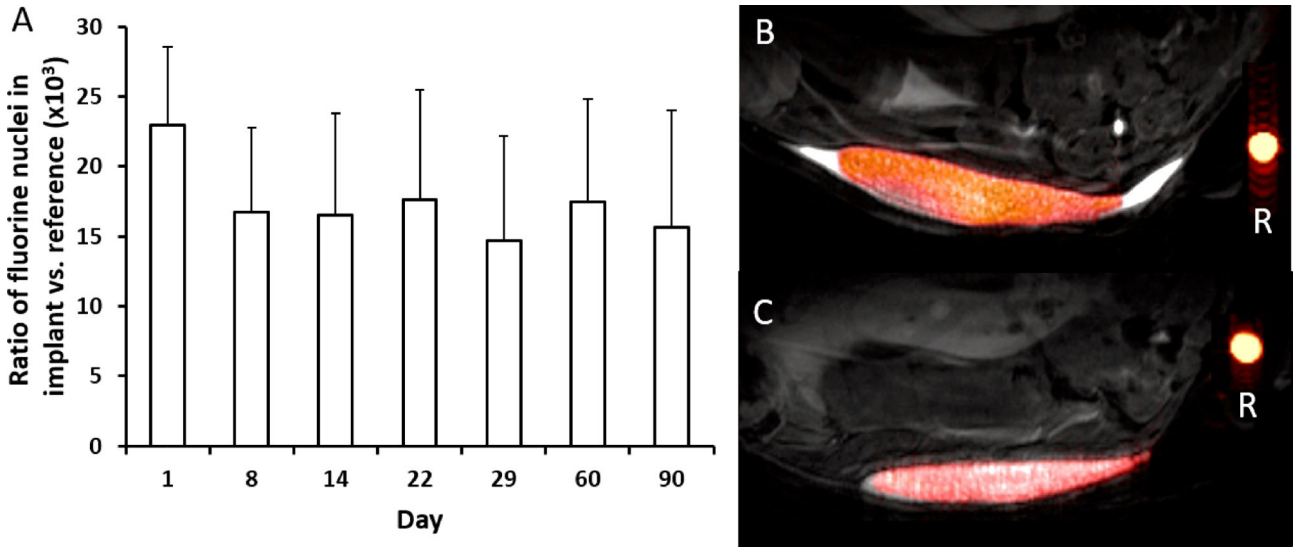

Fig. 3:

S.c. transplantation of 5,000 dual-alginate layer fluorocapsules in C57/Bl6 mice (n=5). a) Total ^{19}F nuclei per voxel in the implant over time, normalized to reference. No significant differences could be observed for 90 days ($p>0.05$). b,c) *In vivo* overlaid ^{1}H/^{19}F MR 11.7T images of s.c. dual-alginate layer fluorocapsule grafts at 1 (b) and 90 days (c) post-transplantation. Reference (R) is undiluted PFPE emulsion.

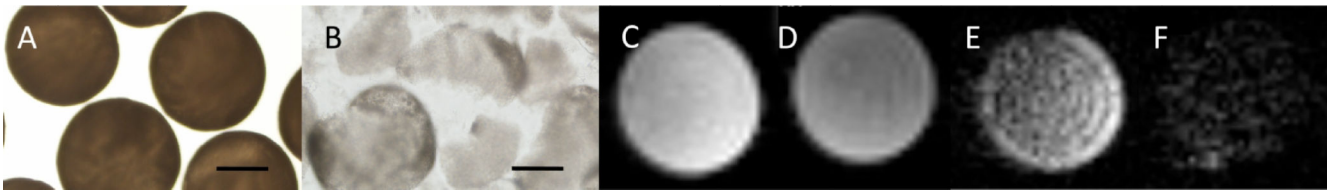

Fig. 4:

Light microscopic images of a) intact and b) ruptured b) single-alginate layer fluorocapsules in saline. Scale bar=200 μm. c,d) Axial ^{1}H and corresponding e,f) ^{19}F MR images at 17.6T of intact (c,e) and ruptured (d,f) fluorocapsules inside 5 mm NMR tubes.

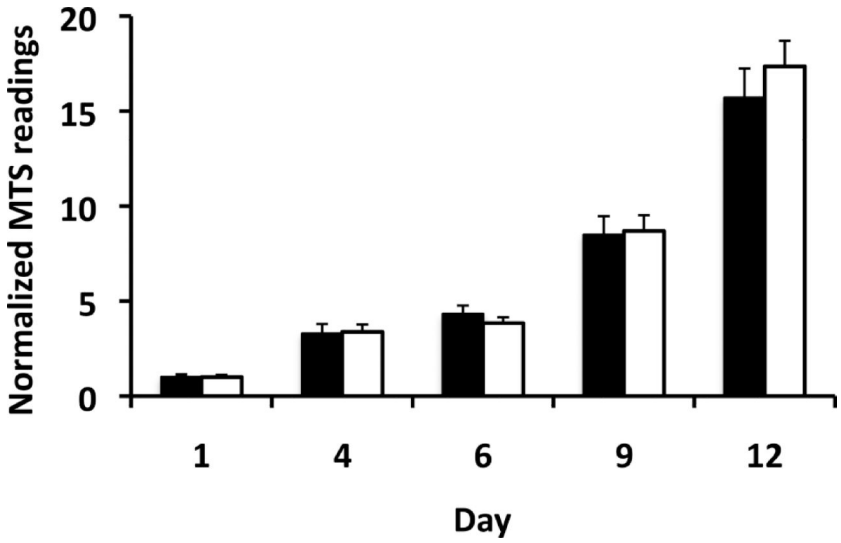

Fig. 5:

MTS assay of mouse βTC6 insulinoma cells cultured without (black bars) and with (white bars) alginate lyase. MTS readout values were normalized against the value at day 1 post-culture. There was no significant difference in cell viability/proliferation over time ($p>0.05$).

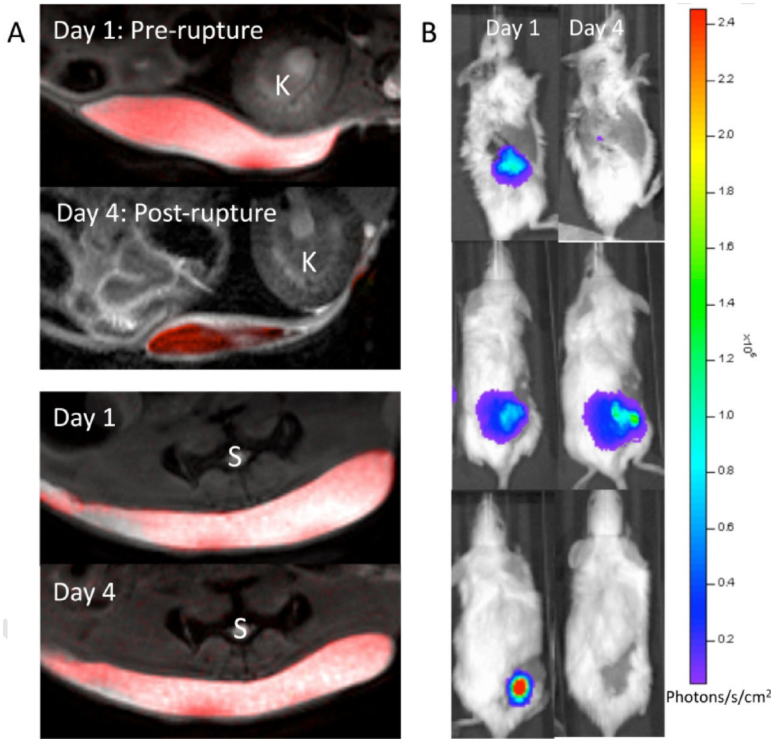

Fig. 6:

a) *In* vivo $^{1}H/^{19}F$ MR images at 11.7T before and after single-alginate layer fluorocapsule rupture by alginate lyase (top panel) vs. control (no alginate lyase, bottom panel). b) Corresponding BLI of mice before and after single-alginate layer fluorocapsule rupture (top panel), without alginate lyase treatment (middle panel), and with naked (unencapsulated) cells (bottom panel). K=kidney, S=spine.

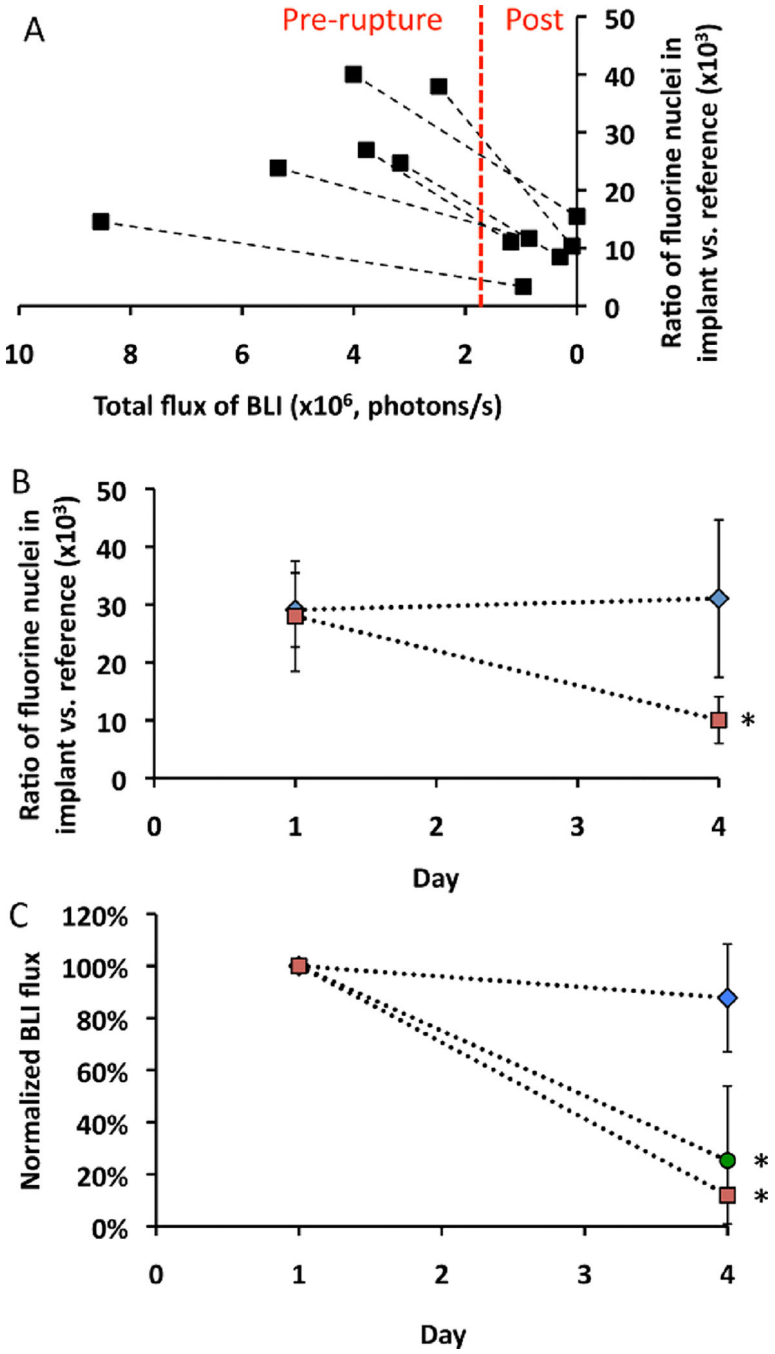

Fig. 7:

a) Correlation plot of ^{19}F signal intensity from implanted single-alginate layer fluorocapsules vs. BLI signal of encapsulated mouse islet cells before and after capsule rupture using alginate lyase (n=6 mice). b) ^{19}F signal intensity of implanted single-alginate layer fluorocapsules with (red symbols, n=6) or without (blue symbols, n=5) alginate lyase injection at day 1 (pre-rupture) and day 4 (post-rupture). c) Normalized BLI signal intensity with (red symbols, n=6) or without (blue symbols, n=5) alginate lyase injection. For comparison, unencapsulated (naked) mouse islet cells (green symbols, n=5) at day 1 (pre-

rupture) and day 4 (post-rupture) are included. The BLI photon flux values were normalized against the values at day 1. Asterisks indicate statistical significance ($p<0.05$).